Steam Gasification of Refuse-Derived Fuel (RDF): Influence of Process Temperature on Yield and Product Composition

ARTICLE *in* ENERGY & FUELS · SEPTEMBER 2006

Impact Factor: 2.79 · DOI: 10.1021/ef060239m

Waste Management 29 (2009) 678–689

Contents lists available at ScienceDirect

Waste Management

journal homepage: www.elsevier.com/locate/wasman

Steam gasification of tyre waste, poplar, and refuse-derived fuel: A comparative analysis

S. Galvagno [a,*], G. Casciaro [b], S. Casu [c], M. Martino [d], C. Mingazzini [e], A. Russo [d], S. Portofino [a]

[a] Department of Environment, Global Change and Sustainable Development, C.R. ENEA Portici, via Vecchio Macello loc. Granatello, 80055 Portici (Na), Italy
[b] Department of Physical Technologies and New Materials, C.R. ENEA Brindisi, SS. 7 Appia-km 706, 72100 Brindisi, Italy
[c] Department of Environment, Global Change and Sustainable Development, C.R. ENEA Bologna, via Martiri di Monte Sole 4, 40129 Bologna (Bo), Italy
[d] Department of Environment, Global Change and Sustainable Development, C.R. ENEA Trisaia, SS 106 Jonica km 419+500, 75026 Rotondella (MT), Italy
[e] Department of Physical Technologies and New Materials, C.R. ENEA Faenza, via Ravegnana 186, 48018 Faenza (RA), Italy

ARTICLE INFO

Article history:
Accepted 2 June 2008
Available online 25 July 2008

ABSTRACT

In the field of waste management, thermal disposal is a treatment option able to recover resources from "end of life" products. Pyrolysis and gasification are emerging thermal treatments that work under less drastic conditions in comparison with classic direct combustion, providing for reduced gaseous emissions of heavy metals. Moreover, they allow better recovery efficiency since the process by-products can be used as fuels (gas, oils), for both conventional (classic engines and heaters) and high efficiency apparatus (gas turbines and fuel cells), or alternatively as chemical sources or as raw materials for other processes. This paper presents a comparative study of a steam gasification process applied to three different waste types (refuse-derived fuel, poplar wood and scrap tyres), with the aim of comparing the corresponding yields and product compositions and exploring the most valuable uses of the by-products.

1. Introduction

In recent years, the quantity of municipal solid waste has increased significantly in the EU and other industrialized countries. Increased consumption has been accompanied by increasing use of high performance articles (with respect to characteristics, esthetic and specificity) with shorter lifetimes. In this framework, the problem of waste management is becoming more and more important, not only for environmental protection but also for maintenance of natural resources. The EU has addressed this problem by utilizing a management hierarchy that favours waste minimization, reuse, recycling, and matter and/or energy recovery, and that considers final disposal as the least preferable option.

Thermal disposal is not only a viable alternative to landfills, but it is remarkable in that it allows the recovery of resources from "end of life" products. Because of its high level of technological development, direct combustion is currently the only commercially available alternative to the landfilling. Nevertheless, due to the limits of recovery efficiency, such technology has many problems related to the control of harmful emissions of acidic gases (SO_x, HCl, HF, NO_x), volatile organic compounds (VOCs), PAH, PCB, PCDD, and heavy metals. An adequate gas treatment system greatly reduces the content of these harmful species to acceptable values, but increases the costs and complexity of the plants; furthermore, the problem of solid residue disposal is still left unsolved.

Besides direct combustion, other emerging thermal treatments, such as pyrolysis and gasification, may represent some effective alternatives to landfilling (Kiran et al., 2000; Galvagno et al., 2002; Morris and Waldheim, 1998; Bridgwater, 2003; Malkow, 2004). Such treatments use less drastic conditions in comparison with the classic direct combustion method, providing for reduced heavy metals gaseous emissions (except for cadmium and mercury); PCDD production is limited as well (Porteous, 2001; Helsen and Van den Bulck, 2005). Moreover, they allow higher recovery efficiency since the process by-products can be used as fuels (gas, oils), for both conventional (classic engines and heaters) and high efficiency apparatus (gas turbines and fuel cells) (Belgiorno et al., 2003; Franco and Giannini, 2005; McKendry, 2002). Alternatively, they can be used as chemical sources or as raw materials for other processes (Wang et al., 2000; Weimer, 1997; Ko et al., 2004; Mui et al., 2004; Napoli et al., 1997; Rodriguez-Reinoso et al., 1995; Pakdel et al., 2001; Elordi et al., 2007).

Recent regulations have introduced the use of RDF (refuse derived fuel) with the aim of standardizing the characteristics of the materials supplied to thermal treatment plants and of improving the whole recovery efficiency. Even if RDF utilization in waste-to-energy plants is still limited, the importance of energy recovery from waste is gaining a fundamental role within the context of conventional energy source crises.

This work presents a comparative study of a steam gasification process applied to three different waste types. The use of poplar

* Corresponding author. Tel.: +39 081 7723578; fax: +39 081 7723344.
E-mail address: sergio.galvagno@portici.enea.it (S. Galvagno).

0956-053X/$ - see front matter © 2008 Elsevier Ltd. All rights reserved.
doi:10.1016/j.wasman.2008.06.003

wood (a biomass), scrap tyres (whose use was defined as a priority objective from the EU community), and RDF is analysed. The processes are conducted using identical conditions on the different materials, and the results are compared with respect to yields and product compositions. Particular attention is paid to the definition of adequate exploitation of the syngas and on determining the most valuable route for solid by-product utilisation.

2. Experimental section

2.1. Materials

The samples used for the experimental work were commercial products provided by Italian suppliers. The samples of RDF, because of their high moisture content (about 25–30%), were first dried and then milled into particles up to 2 mm in diameter. After being ground, they were kept at ambient conditions. About 250 g of material was used for each test.

Samples of poplar wood sawdust were first dried, and then milled into particles up to 4 mm in diameter. After being ground, the samples were maintained at ambient conditions. About 250 g of material was used for each test.

The scrap tyre samples were first dried then shredded to 2 mm diameter particle size. The materials were stored under dry conditions.

2.2. Apparatus and procedures

A schematic diagram of the experimental device is shown in Fig. 1. The gasification tests were carried out on a bench-scale rotary kiln reactor, produced by Lenton (PTF 16/75/610 model). Rotary kilns have not been widely employed for gasification treatment, but they offer flexible configurations able to provide easy management of the process even with a highly heterogeneous material such as RDF (Galvagno et al., 2006).

The material was loaded into a feeder hopper with a maximum capacity of 5 L, fitted with an airtight closure system and a mechanical stirrer. During the experiments, the material was continuously fed to the alumina reactor by means of a screw-driver device, whose rotation was controlled by an inverter. Inside the reactor, the material rolled down the length of the kiln across a series of shields, tilted at 30°, which assisted the transport and limited heat dispersion outside the refractory shell. Feeding started once the reactor reached the temperature selected for the experiment. The kiln rotation speed was adjusted by an inverter, while the reactor slope could be varied up to 10°. The furnace was externally heated and three different thermocouples were provided to measure the temperature axially along the reactor.

The solid residue was continuously discharged into a tank at the outlet of the reactor while the process gas was directed to the cleaning system. The stream passed through an ice jacketed condenser trap that cooled it to room temperature and removed any oil particles from the gaseous products; subsequently, it first bubbled into a 1 M NaOH solution, which acted as a basic scrubber for acid removal, then into a water based bubbling system that prevented any further charcoal transport. The amount of condensation throughout the cleaning system was detected by the weight difference. After treatment, the gas flow was measured by a gas meter before being analyzed and then discharged into the final abatement system. All the characteristics of the experimental device are reported in Table 1.

Gasification tests were carried out with steam produced in a boiler and pumped into the reactors through a peristaltic pump at a fixed flow rate. Nitrogen was used as the carrier gas to create safe working conditions. Before starting the gasification experiments, the initial nitrogen flow rate was maintained at 1.5 L min^{-1} to completely purge the system until the prescribed process temperature was reached.

The gases produced were monitored on-line by process gas chromatography and off line by FTIR analysis performed on discontinuously collected gas samples. The gas heating values were calculated from composition data.

A TA TGA 2950 system, coupled with a thermo optek FTIR spectrometer, was used to set up the thermal process and to characterize the samples with respect to proximate analysis (Mayoral et al., 2001) (that is moisture, volatile matter, fixed carbon, and ash content of the material). Thermogravimetric curves were recorded at different heating rates, using pure nitrogen as an inert purge gas, at a constant flow rate of 100 mL min^{-1}.

The proximate analyses were verified according to the CTI (Italian Technical Committee) Standard 2/156.6 and CT1 2/156.7,

Table 1
Bench-scale plant characteristics

Parameter	Value
Oven heating	Electric, three independent zones
Maximum power	9.2 kW
Maximum temperature	1600 °C
Maximum working temperature	1550 °C
Heating zone length	610 mm
Material reactor	Recrystallized alumina
Reactor length	1550 mm
Inside diameter	80 mm
External diameter	94 mm
Reactor volume	7.79 dm^3
Heating zone volume	3.06 dm^3

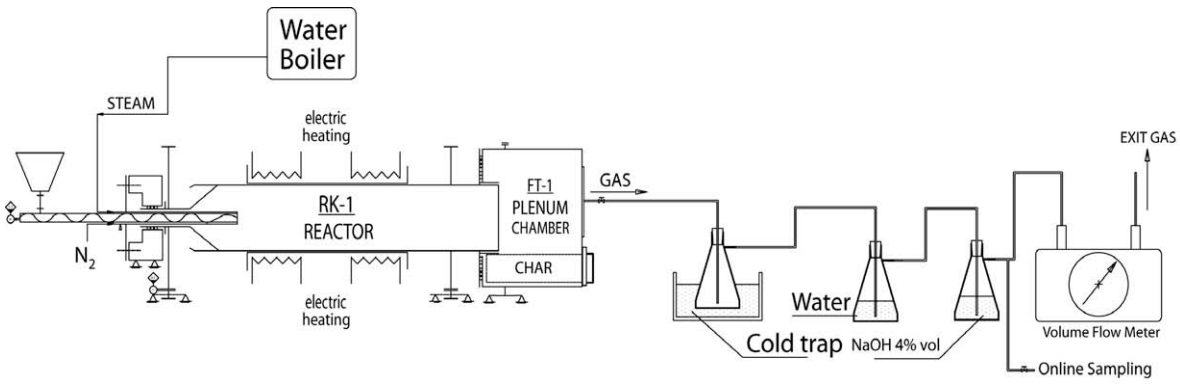

Fig. 1. Schematic diagram of the experimental apparatus.

which specify that volatile content is calculated by burning the sample in a closed metallic pot at 850 °C for nearly 7 min; ash residue is burned further at 750 °C until a constant weight is obtained, and the fixed carbon is obtained by the weight difference. The organic matter is the sum of the volatile fraction plus the fixed carbon. The ultimate analysis was obtained with a Thermo Quest EA 1110 analyzer. Such analysis simultaneously gives the weight percent of carbon, hydrogen, nitrogen, and sulphur in the samples; oxygen determination can be obtained afterwards by the difference.

Specific surface area analyses were performed with a gas sorption analyser (Quantachrome Nova 2000 Model), using gaseous nitrogen as an adsorbate and liquid nitrogen as a coolant. Before measurement, the samples were treated for 6 h in vacuum at 250 °C to remove any physically adsorbed molecules. The data were processed according to the BET equation.

The heating value of the materials was estimated using an IKA C5000 bomb calorimeter in adiabatic modality. Flue gas from the combustion chamber was allowed to pass through a sampling bottle filled with a $NaHCO_3/Na_2CO_3$ buffer solution to be further analyzed for chlorine content.

On-line gas analysis was carried out with a gas chromatograph, model 3000A AGILENT, able to provide precise analysis of the principal gas components (H_2, O_2, N_2, CO, CO_2, CH_4, C_2H_4, C_2H_6) in not more than 2–3 min. The instrument was equipped with two different columns working in parallel (Molsieve 5 A e Poraplot Q) and used a thermal conductivity detector (TCD). The carrier gas was argon in all analyses.

A Stereoscan 250 Cambridge scanning electron microscope (SEM) was used for the product characterization. SEM analyses were conducted on samples of SiC as synthesized.

3. Results and discussions

3.1. Characterization of the starting materials

Fig. 2a, b, and c show TG–DTG profiles of RDF, poplar, and tyres, respectively, recorded in the nitrogen atmosphere heated to 900 °C at a constant heating rate of 20 °C/min, followed by air combustion. The experimental configuration, including the coupling of the thermobalance with a FTIR spectrometer, allows the simultaneous characterization of the gaseous decomposition products (Fig. 3a–c). The figures show several prominent spectra extracted from the FTIR series for the three materials.

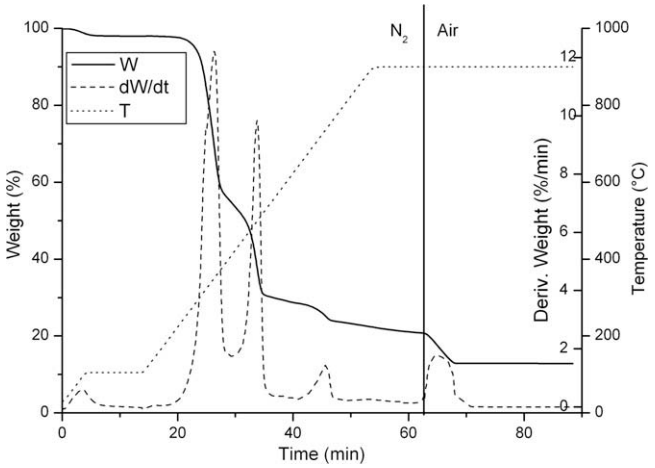

Fig. 2a. RDF Thermogram; ramp at 20 °C/min in N_2 to 900 °C, followed by air combustion.

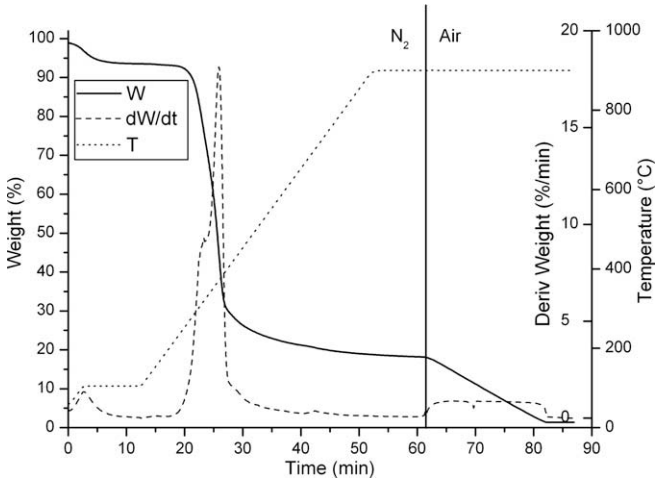

Fig. 2b. Poplar wood thermogram; ramp at 20 °C min^{-1} in N_2 to 900 °C, followed by air combustion.

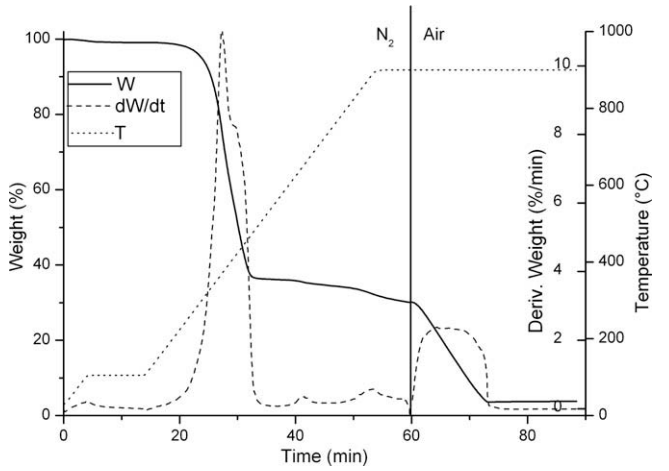

Fig. 2c. Waste tyre thermogram; ramp at 20 °C min^{-1} in N_2 to 900 °C, followed by air combustion.

Thermal analysis has been widely used in pyrolysis research to investigate kinetic parameters such as activation energy and reaction order, and to attempt the identification and quantification of the evolved chemical species to allow the formulation of a thermal degradation mechanism (Garcia et al., 1995). This last aspect was particularly supported, in our experiments, by the FTIR analyses of the evolved gas. In this respect, Table 2 lists the main compounds revealed by the registered spectra and the corresponding main FTIR signal ranges. The identification was made directly on the acquired spectra by using the best match criteria of the Aldrich Vapour Phase Library and the HR Nicolet TGA Vapour Phase Library. In addition, the signal attribution was compared with data from the literature (Lu et al., 1996, 1999; Bassilakis et al., 2001; Xie et al., 2001).

With respect to RDF, the decomposition takes place through a series of complex peaks related to the simultaneous degradation of the various fractions (paper, plastics, wood, and fabrics) which make up the material. Three main mass loss stages are found; the DTG curves show that the maximum pyrolysis reaction rate occurred at 312–360 °C in the first reaction, at 430–540 °C in the second reaction and above 650 °C in the last reaction. The comparison with TG curves for the pyrolysis of materials such as paper, LDPE, and wood, and the analysis of evolved gas from FTIR (Fig. 3a) let

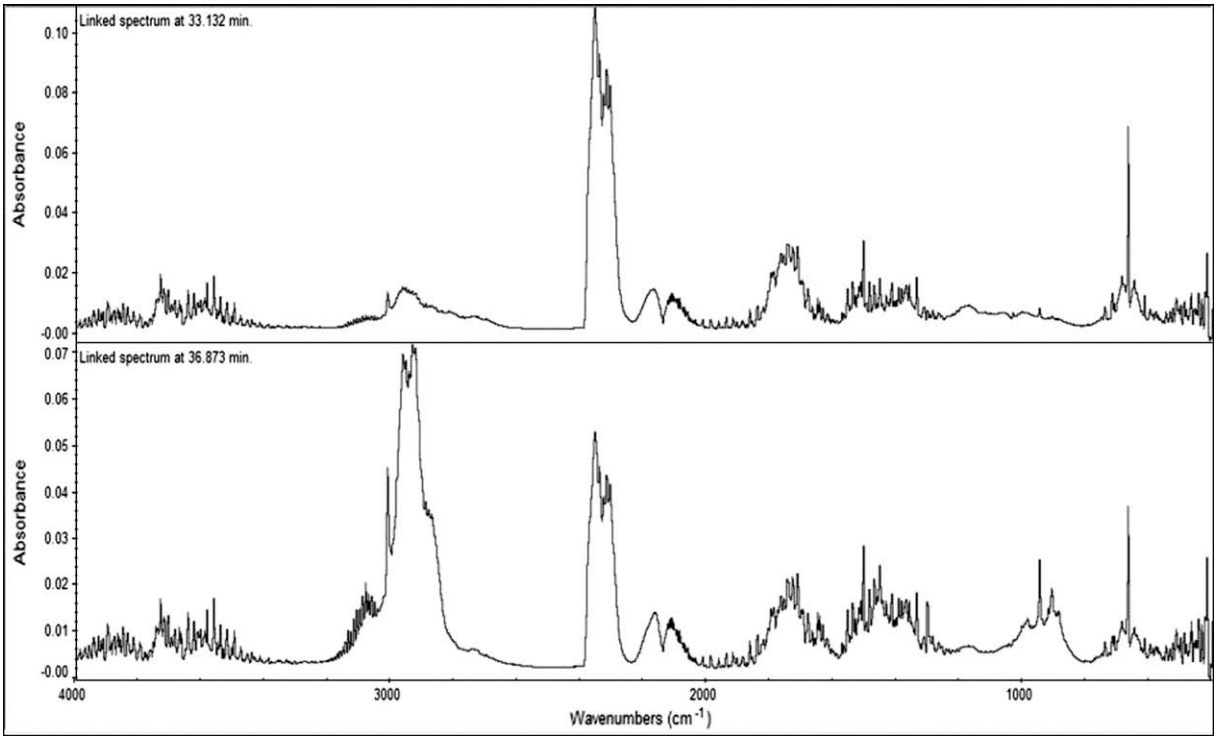

Fig. 3a. FTIR series of RDF product decomposition.

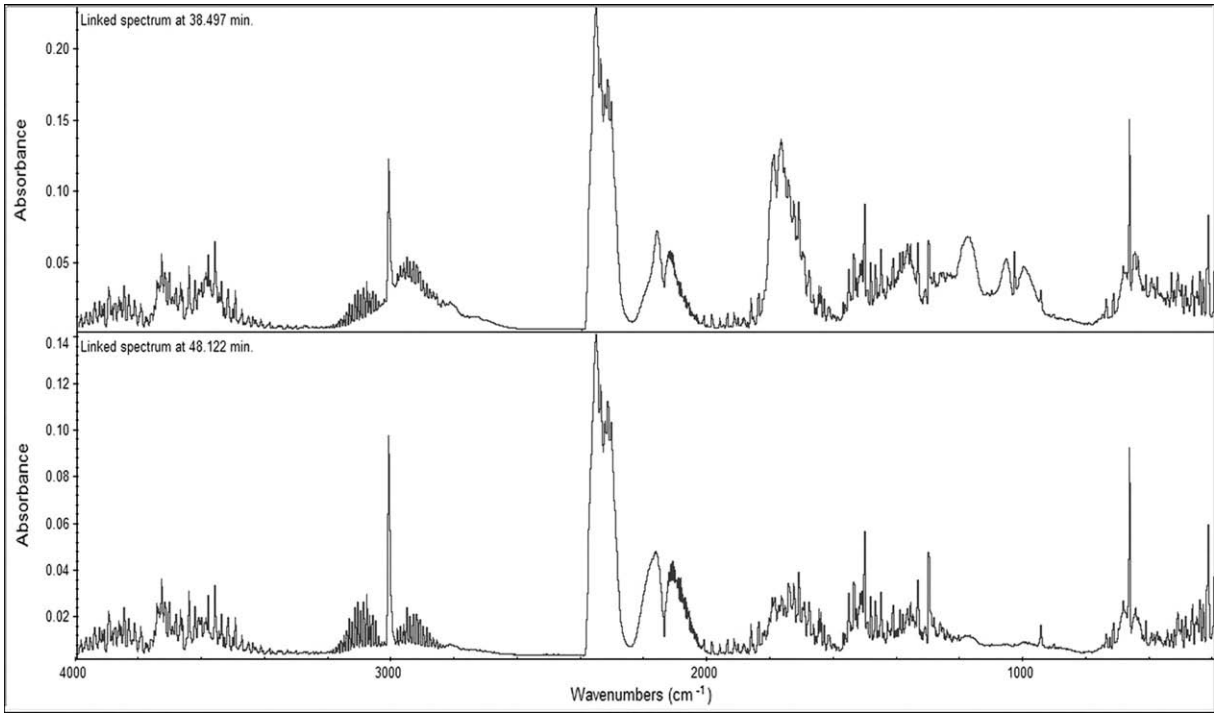

Fig. 3b. FTIR series of poplar product decomposition.

us ascribe the first and the third peak to the decomposition of cellulose and ligneous materials (with the detection of CO_2, methanol, acetic acid, and acetaldehyde in the FTIR series); the second peak is most likely due to the decomposition of plastics, mainly LDPE, as confirmed by the FTIR spectra of ethylene, propylene, methane, and other aliphatic compounds (Casu et al., 2005; Cozzani et al., 1995).

With respect to poplar (Fig. 2b), the peak at the higher temperatures is mainly due to the decomposition of cellulose (Stenseng et al., 2001), and the shoulder at lower temperatures can be attributed to the decomposition of hemicellulose, as confirmed by the corresponding FTIR signals of the main decomposition products (formaldehyde, hydroxyacetaldehyde, CO and CO_2; Banyasz et al., 2001). The lignin contribution is distributed over a large range of

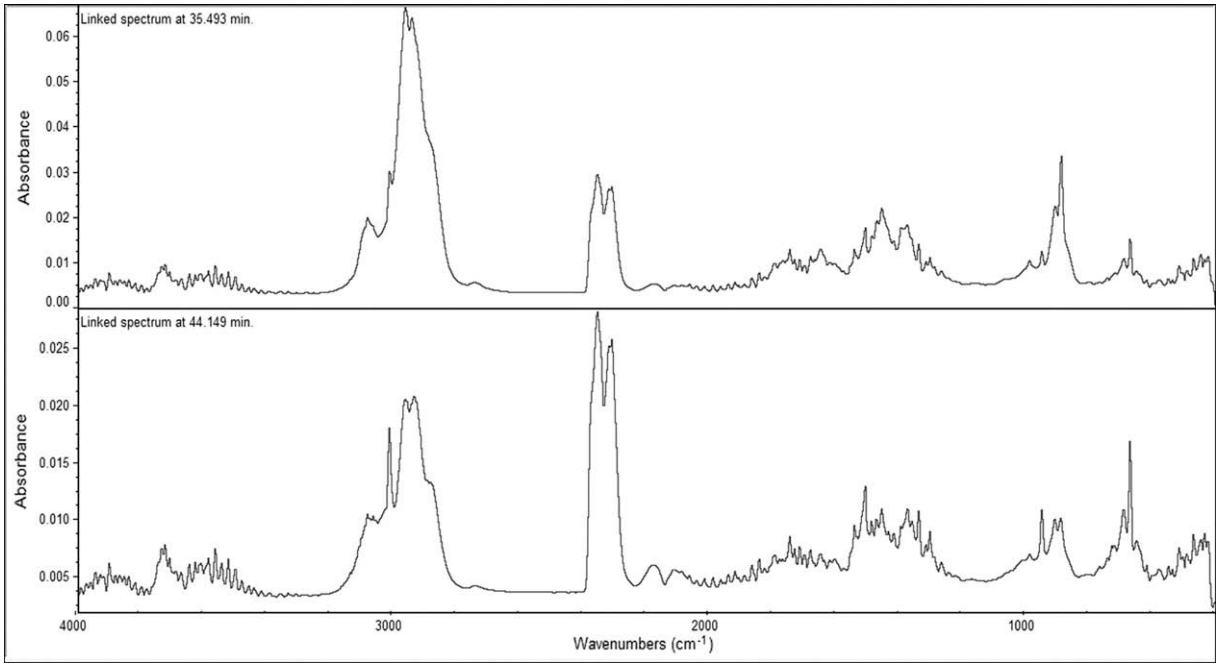

Fig. 3c. FTIR series of scrap tyre product decomposition.

Table 2
FTIR signals of functional groups and species

	Main FTIR signal (cm^{-1})
Water	3790
Carbon monoxide	2120–2180
Carbon dioxide	2360–2335
Methanol	1032
Ethanol	1760
Ethanoic acid	1796
Methane	3016, 1305
Ethylene	949
Propylene	911
Acetylene	729
Carbonyl Sulfide	2062
–CH aliphatic	2930–2970
Benzene and aromatics	3060–3080, 1480, 1040, 670
2-Methyl-1,3-butadiene	2986, 905
Cyclohexene	2935

temperatures and overlaps with previous components (Varhegyi et al., 1997).

The decomposition profile of the tyre waste (Fig. 2c) shows that the thermal decomposition starts at about 220 °C and is practically complete at ~600 °C. The decomposition occurs through a series of peaks which account for the simultaneous degradation of the main components of the tyre, principally natural rubber (NR), styrene-butadiene rubber (SBR), and butadiene rubber (BR). The maximum degradation rates are in the temperature range of 375 °C for NR, 445 °C for SBR, and 465 °C for BR. Despite the presence of a complex mixture, the analysis of the volatile products via FTIR could be the basis of distinguishing the contribution of the different elastomers to tyre degradation (Williams and Besler, 1995; Galvagno et al., 2007), following the trend of decomposition of NR by the signals of 2-methyl-1,3-butadiene, the trend of decomposition of BR by butadiene and cycloheptadiene, and the trend of decomposition of SBR by toluene and benzene. Even the spectra extracted from the FTIR characterization of our samples, shown in Fig. 3c, reveal the presence of such classes of compounds (particularly the peak at 906 cm^{-1} for 2-methyl-1,3-butadiene and the aromatic range of bending at 1450–1600 cm^{-1}). Sets of formal kinetic parameters can be found in the literature for the different rubber types and for their mixtures (Leung and Wang, 1998; Sułkowski et al., 2004), and these parameters vary in their dependence on the experimental equipment and the mathematical treatment of the obtained data.

Proximate analysis is a standard compositional analysis conducted for the determination of moisture, volatile matter, fixed carbon, and ash of compounds, and is used to establish the rank of coal and to show the ratio of combustible to incombustible constituents. While the volatile matter (often comprising the moisture) generally accounts for the fraction that evolved by thermal decomposition, the fixed carbon, together with the ash, represents the theoretical solid residue (the char fraction) of a possible pyrolysis/gasification process. In this respect, the data in Table 3 provide a comparative frame of the different feedstocks and give a clear indication of the corresponding thermal behaviour.

All the materials present very high volatile contents (60–80%); with respect to the solid residue, the yield is comparable for poplar and RDF (≈20%), while it is much higher for tyres. Nevertheless, an in-depth study of char shows that the ash represents the majority of the solid residue in RDF, while the ash content in poplar is almost 1.7%.

Table 3
Proximate and ultimate analyses of starting materials

	RDF	Poplar	Tyre
Proximate analysis (wt% dry basis)			
Volatile matter	79.7	81	61.8
Fixed carbon	6.8	17.3	33.8
Ash	13.5	1.7	4.4
Ultimate analysis (wt% dry basis)			
C	48.8	47.5	85.2
H	7.8	6.1	7.3
N	0.7	0.1	0.4
S	0.0	0.0	2.3
O[a]	29.2	44.6	0.5
GHV (MJ/kg)	19.9	19.0	37.1

[a] By difference.

The data show that tyres have the highest carbon content, and result in a high fixed carbon in the char, and a hydrogen content of 6–8%. Moreover, due to the vulcanization process of the rubber, the presence of sulphur is remarkable into the tyre composition (~2.3%), while it is negligible in poplar, as expected and in RFD, where it is mainly ascribed to the contribution of the plastic fraction. The oxygen, measured by difference, varies from 43% (poplar) to 0.5% (tyre). Consequently, the heating value is higher for scrap tyres than for both poplar and RDF, which show almost constant oxygen values. There is no evidence of chlorine, as shown in both the spectrometric FTIR measurements and the combustion and flue gas analysis.

3.2. Gasification tests

Gasification tests were conducted with steam holding all operational parameters constant, including the temperature (850 °C), the steam/material ratio, and the residence time inside the reactor. Table 4 presents the operating parameters.

The repetition of the experiments provided reproducible and coherent data.

The flow of a material through a rotary kiln is determined by the kiln's slope and the rotational speed, as well as by the characteristics of the material being processed. The kiln is installed on a slight slope so that the bed of solids advances by the force of gravity; as the kiln rotates, the material follows the rotation until it breaks the surface of the bed and tumbles down the sloping surface. The kiln residence time (t_s) is expressed by the formula (Sullivan et al., 1927):

$$t_s = (1.77 * (\sqrt{\theta}) * B * L)/(S * N * D)$$

where θ is the dynamic angle of repose (dependent on the material), L is the kiln length, B is the correction factor (equal to 1 for undammed kilns, >1 for dammed kilns), S is the kiln slope, N is the rotational speed of the kiln, and D is the inside diameter of the reactor. The dynamic angle of repose of the material, which is the constant slope of the bed surface, affects the time required to transport the material through the kiln, and therefore affects the kiln residence time and is dependent upon the material characteristics and the slope.

The gas residence time (t_g) is calculated assuming an ideal behaviour, according to:

$$t_g = V/F_T$$

where V is the heating zone volume and F_T is the flux at the processing temperature.

Under these conditions, the yields of the various fractions (char and gas) for the gasification trials are reported in Table 5 with respect to the different materials.

As expected, the sum of the yields of the various fractions, compared to the incoming feedstock, exceeds 100% in any individual test because of the contribution of steam to the reaction (Wie et al., 2007). The data account for a negligible contribution of the liquid fraction; it is important to note that the oil fraction was determined by weight difference of the cold trap, and no evidence of condensed matter was observed elsewhere in the cleaning system. On the other hand, data from the literature for biomass gasification (Turn et al., 1998; Wie et al., 2007; Kamo et al., 2006), which was performed under quite similar experimental conditions, showed an average yield of ~7–10 g tar/kg of biomass, which accounts for <1% of the fuel mass.

Poplar produces the highest gas yield and the lowest char yield, while char yields of waste tyres and RDF are comparable. Nevertheless, considering the ultimate analysis of the different types of char (Table 6), some essential differences result regarding the composition of the solid residue.

Table 4
Operating parameters of the kiln gasification reactor

Parameter	Value
Temperature	850 °C
Pressure	1.02 bar
Steam partial pressure	0.8 bar
Rotational speed of reactor	2 rpm
Reactor slope	3°
Gas flow (N_2)	2 dm^3 min^{-1}
Feeding rate	1.17 g min^{-1}
Steam flow rate	2.60 g min^{-1}
Steam/biomass ratio	2.21
Solid residence time	15 min
Gas residence time	9 s

Table 5
Fractions yields

	Char yield (% w/w)	Gas yield (% w/w)
RDF	36.0	81.3
Poplar	14.4	89.9
Tyre	41.2	60.8

3.3. Char analysis

Unlike waste tyres, char from RDF is largely composed of ash and its further exploitation as a secondary row material for high added value products (carbon source, active carbon) is limited. Nevertheless, some interesting applications can be found even for this kind of char, such in polishing media, roofing granules, landscaping, road surface coating, and as a cement additive to improve the properties of concrete in construction materials (Hwang et al., 2007). From the standpoint of fuel recovery, it seems more attractive to use these materials in the gasification process, in order to produce greater gas production (Chaudhari et al., 2001; Braekman-Danheux et al., 1998,). The other two materials instead show high organic contents, together with small ash contents, which make them suitable for other applications. Moreover, the similarity between poplar and RDF with respect to the char organic content, whose value becomes 13.4% (for poplar) and 12.0% (for RDF) if normalised against the char yields (36.0% and 14.4%, respectively), is notable; this result, together with the similar volatile content on the starting material (see Table 3), suggests that the RDF composition accounts for a high lignocelluloses fraction. Conversion, reported in Table 6, is calculated according to the following formula:

Table 6
Char characteristics

	RDF	Poplar	Tyre
Proximate analysis (wt% dry basis)			
Ash	66.8	6.8	9.0
Organic	33.2	93.2	91.0
Organic[a]	12.0	13.4	37.5
Conversion	0.86	0.86	0.61
Ultimate analysis (wt% dry basis)			
C	18.5	85.8	82.7
H	0.7	1.1	1.0
N	0.2	0.1	0.2
S	0.0	0.0	3.0
O[b]	13.8	6.2	4.1
H/C	0.038	0.013	0.012
Specific Surface Area (m^2/g)	12	104	40

[a] Calculated over the total, considering the char yield.
[b] By difference.

conversion = reacted organic matter/total organic matter

Accordingly, conversion for poplar and RDF is almost coincident, while for waste tyres conversion is still low under the adopted operating conditions.

Regarding the ultimate analysis, the data show a high carbon content for poplar and tyres, while in char from RDF the carbon percentage is considerably lower and the ash content is very high (see Table 6). Furthermore, the hydrogen content is nearly constant for the three materials (~1%).

The H/C (hydrogen-to-carbon) ratio provides an indication on the insaturation grade of a material, and for this reason, it is normally used as an indicator for coal ranking: the lower the H/C ratio, the higher the quality of the coal. In the chars in this study, the very low H/C ratio depends upon the high extension of the cracking reactions of the material during the gasification process; a graphite-like structure is expected at the working temperatures of our tests, since it is known that the char can undergo rearranging reactions with the contemporaneous removal of small molecules such as CO or CH_4 (Sharma et al., 2001).

Only char from tyres shows a high sulphur content (~3% by weight). Considering a sulphur content of 2.3% by weight on waste tyre feeding and a char yield of 41.2% by weight (as shown in Table 5), it is evident that a normalised final 1.2% *S* by weight (almost 50% of the starting sulphur) is retained in the solid residue for the thermally processed tyres.

Specific surface areas, determined by the BET analyses, are very low (Table 6), particularly for RDF, but the measure is largely affected by the high ash content, while for poplar and tyre the very low values could be ascribed to the presence of a graphite-like structure, as suggested by the H/C ratio values.

3.4. Gas analysis

Fig. 4 shows the syngas composition as obtained from online gas chromatographic analyses. The hydrogen content increases in the sequence RDF < poplar < tyres, increasing from 42.7% to 51.5%. Poplar syngas has the highest content of oxygenated products (CO, CO_2), whereas waste tyre syngas has the highest methane, ethylene, and ethyne contents, and is the only one with an appreciable C_3 content (nearly 1%; not reported in Fig. 6).

Obviously, such a trend is dependent upon the different compositions of the starting materials. The presence of highly oxygenated species, such as cellulose and hemicellulose in the poplar, favours the development of large quantities of oxygenated products (Encinar et al., 2002; Franco et al., 2003). In the waste tyres, the high hydrocarbons content depends on the rubber degradation process. RDF presents an intermediate situation, being rich in oxygenated products, probably due to the presence of paper and wood into the waste, and at the same time containing appreciable quantities of methane and ethylene, coming from the degradation of the plastic fraction (Casu et al., 2005).

Generally, the presence of significant amounts of methane, unsaturated C_2 (ethylene and acetylene), and ethane (and C_3) indicates limited extensions of the steam cracking processes into the gas phase, whatever the nature of the material (Turn et al., 1998; Morf et al., 2002). A major gas phase cracking extension can be realised by increasing the steam/material ratio (equal to ≈2 in our experiments). Moreover, the syngas obtained in the different tests is rich in CO, which could be easily converted to additional hydrogen (if a hydrogen rich syngas is desired) by reacting according to the water gas shift reaction (Effendia et al., 2005):

$$CO + H_2O \rightarrow CO_2 + H_2 \quad \Delta H_{298\,k} = -41.2\ \text{kJ mol}^{-1}$$

The water gas shift reaction is a well known reaction in the literature as well as in industrial practice, including syngas production from methane steam reforming processes, and the related processes of feedstock preparation for ammonia synthesis, Fisher–Tropsch synthesis, and coal gasification.

Additionally, the Boudouard reaction:

$$C + CO_2 \rightarrow 2CO \quad \Delta H_{298k} = +172.5\ \text{kJ mol}^{-1}$$

could be used as an alternative treatment to the catalytic upgrading, to change the syngas composition and, of course, the H_2/CO ratio (which we will discuss later). With respect to our process, both the reactions represent possible routes to be followed for gas conditioning to create a hydrogen-rich syngas composition.

In Table 7, the data concerning the gas composition of our experimental tests on poplar gasification are compared to some results from the literature on biomass gasification. As can be observed, the values agree fairly well with the results of Turn et al. (1998), which were collected at a comparable steam/biomass ratio; the different H_2 and CO contents can easily be ascribed to the different advancements of the water gas-shift reaction, which supports the formation of H_2 at the expense of CO. The considerable differences with the results of Franco et al. (2003) are, on the con-

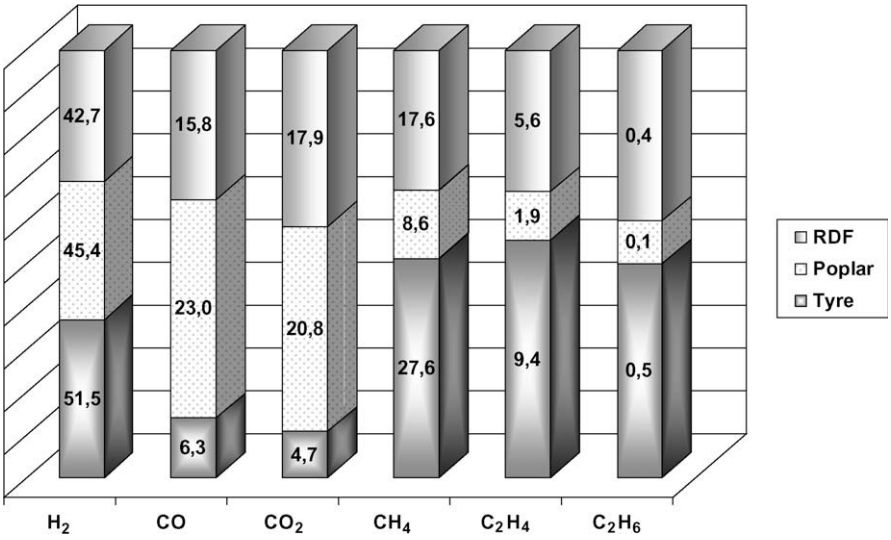

Fig. 4. Syngas composition (% v/v).

Table 7
Gas composition and comparison with data from the literature

	Turn et al. (1998)	Franco et al. (2003)	This work
H_2 (%)	51.3	35	45.5
CH_4 (%)	6.1	10	8.6
CO (%)	15.9	30	23.1
CO_2 (%)	25.1	20	20.8
C_{2ins} (%)	1.7	2.5	1.9
C_2H_6 (%)	–	–	0.1
H_2/ CO	3.2	1.2	2.0
Steam/biomass ratio	1.8	0.8	2.2

trary, attributed to the low steam/biomass ratio (0.8) adopted by those authors.

The literature concerning experimental results on steam gasification of other materials (tyres and RDF) is very sparse; thus, comparisons for these materials were not possible.

The on line chromatographic analyses on the produced syngas were confirmed by the off-line FTIR analyses of the gaseous streams, conducted by sampling the flow during the different tests. The corresponding spectra are shown in Figs. 5a, 5b and 5c.

The FTIR spectra confirm the presence of the gas component monitored by GC, mainly CH_4 (3016 cm^{-1}, 1305 cm^{-1}), CO (2120 cm^{-1}, 2180 cm^{-1}), CO_2 (2360 cm^{-1}, 2335 cm^{-1}), and small saturated and unsaturated hydrocarbon molecules (2930–2970 cm^{-1} for CH_2 and CH_3 stretch, 949 cm^{-1} for ethylene, 729 cm^{-1} for ethyne). Of course, the hydrogen is FTIR transparent. Furthermore, the spectra revealed the presence of benzene (and probably other aromatic species), which were not detected by means of chromatography, in the shoulder around 3060–3080 cm^{-1} and in the peaks at 1480 cm^{-1} and 670 cm^{-1}. Even if FTIR detection does not allow any quantitative evaluation, it reveals that the benzene signals are stronger for tyre syngas, in comparison with RDF and poplar (Lu et al., 1999; Jess, 1996).

Moreover, there is no evidence in the spectra of hydrogen sulfide or sulfur dioxide, pointing out the good efficiency of the abatement system. Such efficiency was confirmed by the examination of a yellow spongy precipitate, probably sulfur, throughout the system. However, it is not possible to exclude the presence of sulphurated compounds into the gaseous flux, since the presence of steam could favour the formation of COS, whose FTIR signal (2062 cm^{-1}) is not easily differentiated from CO signal (Kagann, 1982).

The H_2/CO ratio is a useful indicator for the suitable application of the flue gas. Syngas that has a H_2/CO ratio higher than two is favourable for producing hydrogen for ammonia synthesis or for fuel cell applications (Chaudhari et al., 2001; Lobachyov and Richter, 1998), whereas synthesis gas that has a H_2/CO molar ratio in the range of 1–2 is highly desirable as feedstock for Fischer–Tropsch synthesis for the production of transportation fuels (Hamelinck et al., 2004). As shown in Table 9, the H_2/CO ratio for tyre syngas is 7.8, indicating its potential use as a fuel cell supply, at least in principle.

The situation is not so clear with respect to the other two materials, and in fact for poplar and RDF (with H_2/CO ratios of about 2.0), the syngas could be properly conditioned or upgraded for use in either the fuel cell applications or the chemical synthesis.

Syngas production is practically constant for the three different materials, even if poplar and RDF show gas density of comparable values whereas syngas from tyres is lighter (because of the higher hydrogen content). Syngas from poplar shows the lowest heating value, while the heating value from syngas from tyres is very high.

In terms of energy exploitation of the process, the last column of Table 8 reports the energetic content of the gas, or the energy (expressed in MJ) of the syngas for 1 kg of feeding. The heating values are quite low, well below that of natural gas. The energy content rises in the order poplar > RDF > tyres and depends on the amount of oxygenated compounds (especially carbon dioxide) and on the hydrocarbon content (i.e., methane). Poplar syngas has higher amounts of CO and CO_2 and a lower methane concentra-

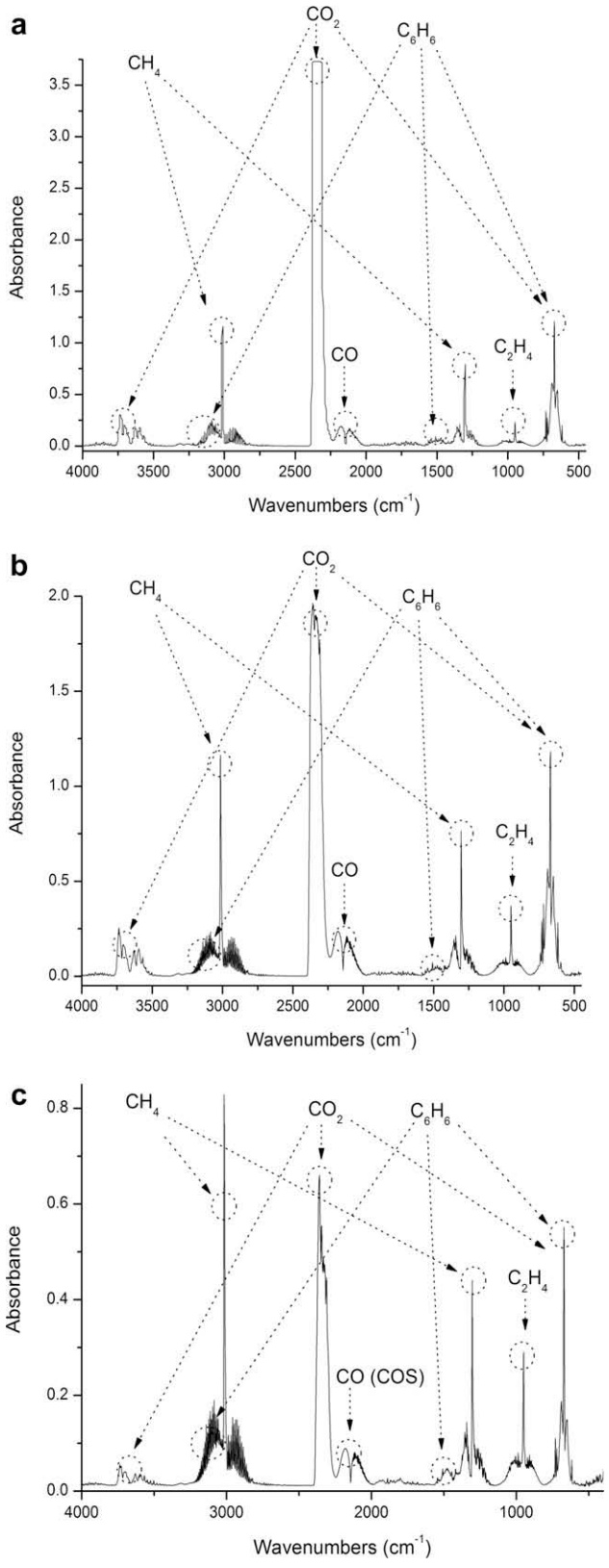

Fig. 5. FTIR spectra of syngas: (a) RDF, (b) poplar and (c) tyres.

Table 8
Syngas characteristics

	Density (kg/m^3)	Gas production (m^3/kg of fed)	Heating value (MJ/m^3)	Energy content (MJ/kg of fed)
RDF	0.79	1.03	17.80	18.33
Poplar	0.82	1.10	13.40	14.70
Tyre	0.55	1.09	25.33	28.12

Table 9
Gas composition (nitrogen-free)

	O_2 (m^3/kg)	H_2 (m^3/kg)	CO (m^3/kg)	CO_2 (m^3/kg)	CH_4 (m^3/kg)	C_2H_4 (m^3/kg)	C_2H_6 (m^3/kg)	C3 (m^3/kg)	Tot (m^3/kg)	H_2/CO
RDF	0.00	0.44	0.16	0.18	0.18	0.06	0.00	0.00	1.03	2.7
Poplar	0.00	0.50	0.25	0.23	0.10	0.02	0.00	0.00	1.10	2.0
Tyre	0.02	0.55	0.07	0.05	0.29	0.10	0.01	0.01	1.09	7.8

tion, while the tyre syngas is the opposite situation, and RDF syngas has intermediate values.

Table 9 gives also the detailed gas composition, expressed as gas volume per kilogram of feeding.

Gas from tyres has the highest hydrogen content, followed by the poplar, and is rich in methane. The poplar syngas shows the highest levels of oxygenated compounds (CO and CO_2), while RDF syngas has intermediate levels.

3.5. Solid by-product exploitation – SiC Synthesis

The industrial applications of the thermal technologies devoted to waste vaporization are strongly limited by the final use of the solid residue, which can greatly affect the overall economic balance of the process. Char produced from waste could be used for many purposes, such as adsorbents, soil conditioners, or alternative fuel, according to its characteristics (composition, heating value, ash content). In this respect, we followed a different approach, considering the char as a low-cost carbon source, to replace coal in chemical reactions, for the production of ceramic materials.

Experiments were conducted on poplar char, which was used for the carbothermal synthesis of silicon carbide. Silicon carbide (SiC) is one of best materials for advanced applications (Wesch, 1996). Its peculiar properties, such as high hardness and strength, excellent corrosion/oxidation resistance, good high-temperature strength, and high thermal conductivity, make it an optimal choice as reinforcement for ceramic composites (Fujisawa et al., 2004).

Methods of synthesizing SiC powders include direct carbonization of Si metals, CVD from silane, sol-gel of silicon alkoxides, and carbothermal reduction of SiO_2. In terms of economy and efficiency, the carbothermal reduction is the best choice. It involves inexpensive silicon dioxide and carbon (or carbon precursors) as the starting materials (Krstic, 1992; Wei, 1983; Krishnarao and Subrahmanyam, 1996), according to the following overall reaction:

$$SiO_2(s) + 3C(s) \Longleftrightarrow SiC(s) + 2CO(g)$$

The synthesis was conducted starting with a mixture of silica and char from poplar, in a tubular furnace at 1550 °C in a dynamic argon atmosphere. The argon flow was set at 0.80 dm^3 min^{-1} in order to support CO elimination during the synthesis, moving the equilibrium of the reaction towards formation of the products with limited SiO removal. Such a gas flow value was set accordingly to data from the literature data and with the aim of achieving a compromise between avoiding a loss of gaseous SiO and the need to effectively remove CO.

The use of poplar char as a carbon source is particularly important, since the process of ceramization of wood or of other biological structures is currently being studied as an attractive way to product porous components with peculiar microstructures which cannot be obtained by other processes (Esposito et al., 2004)The XRD pattern of the resulting SiC product is shown in Fig. 6.

In the figure, the peaks for the β-SiC phases are observed (in particular the (1 1 1) line of the cubic structure of the silicon carbide at $2\theta = 35.64°$ ($d_{111} = 0.251$ nm)), together with the peaks of a second α-SiC phase (mainly the peak at $2\theta = 33.82°$ ($d = 0.265$ nm), which is characteristic of hexagonal polytypes (α-SiC phase)); this indicates that the carbothermal reduction reaction to form SiC occurs with the minor production of a certain amount of α-SiC. Furthermore, the high background noise and the signal widening reveal the presence of an amorphous phase, probably residual silica (Qian et al., 2004b; Qian and Jin, 2006; Kim et al., 2006; Kingetsu et al., 1998). Fig. 7 shows the SEM micrographs of the starting mixture and the as-synthesized SiC.

The micrograph of the starting mixture (Fig. 7a) shows a homogeneous distribution, with light (silica) and grey (carbon) particles representative of the adequate blending of the reagents, which is an essential requirement for the subsequent synthesis. The ceramic product (Fig. 7b) is very similar to the starting carbon, with respect to both shape and morphology (Qian et al., 2004a; Sujirote and Leangsuwan, 2003).

Normally, wood has a strongly anisotropic cellular structure, with the majority of the pore channels oriented along one axis; nevertheless, despite the similarities, each wood has specific properties, which can be transferred to the corresponding ceramic products and which could allow different applications, including filters, catalyst carriers, or multifunctional membranes in case of homogeneous pore sizes, and biocatalyst support in the food industry or waste water treatment for heterogeneous structures (Greil et al., 1998).

With respect to our data, the results are particularly interesting, since poplar is cheap and the gasification process can be applied to many types of waste wood, which can give rise to very different carbon templates useful for the further ceramization process. Due to attention paid to the optimisation of the synthesis process, the relationship between the reactivity of the carbon substrate and the kind of ceramic products the materials could be used for require further investigation.

3.6. Solid by-product exploitation – preparation of activated carbons

Most activated carbon used industrially is produced from natural raw materials like coal, oil, peat, and wood, and they have been thoroughly investigated. Considering the practical use of waste materials as a precursor for industrial activated carbon, additional investigations should be performed to optimize their properties as adsorbents (Nakagawa et al., 2002; Mui et al., 2004; González et al., 2006).

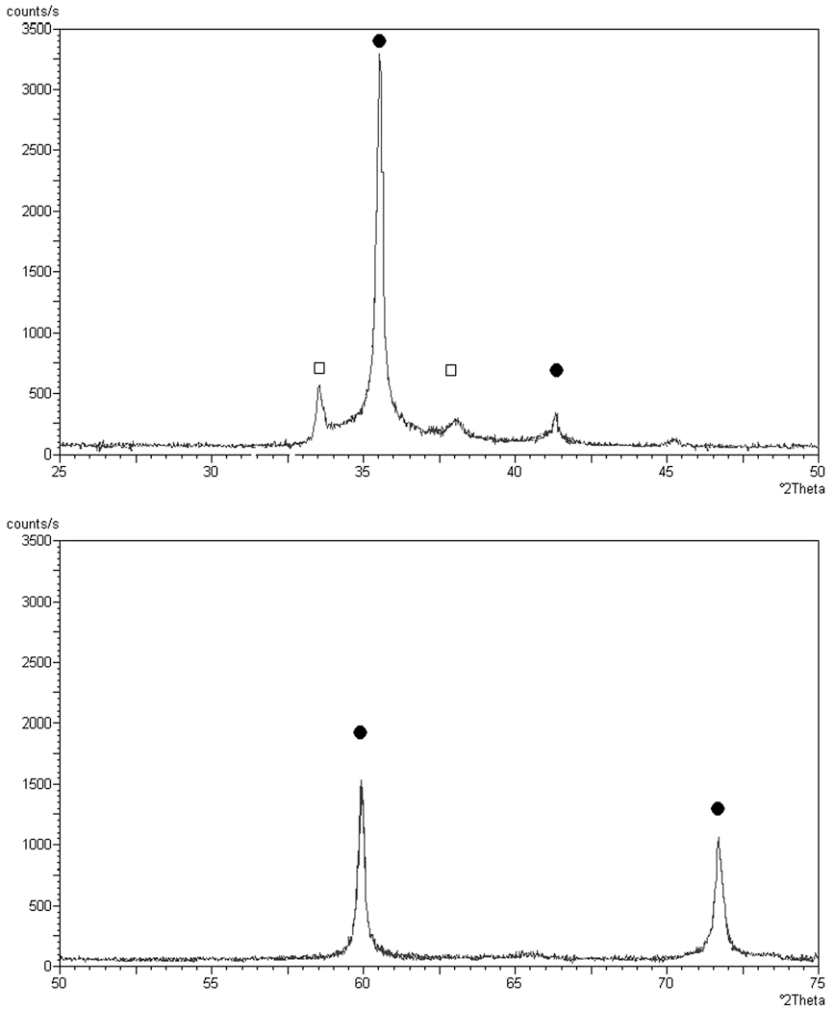

Fig. 6. XRD pattern of the SiC from carbothermal reduction of poplar char, □ α -SiC, ● β –SiC.

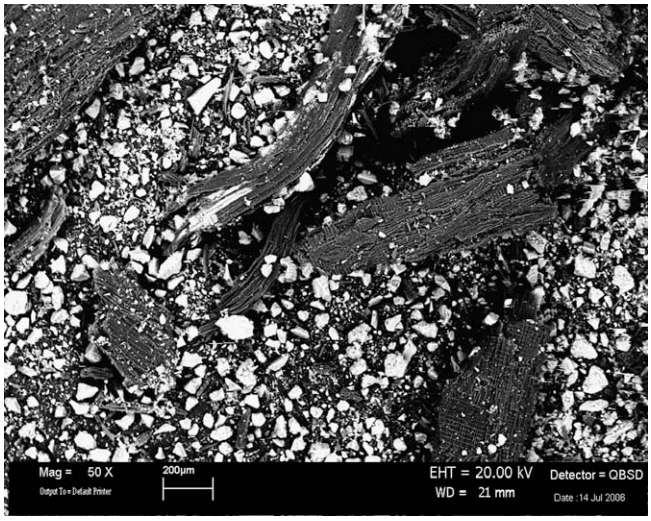

Fig. 7a. SEM micrograph of the starting mixture.

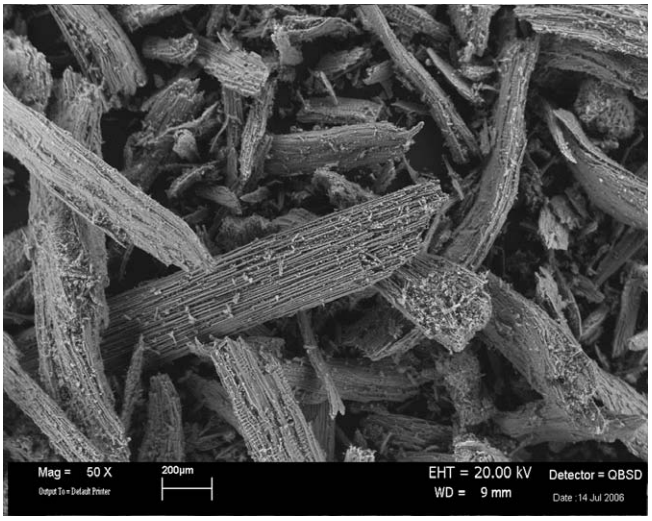

Fig. 7b. SEM micrograph of the as-synthesized SiC.

In this paper, activated carbon was prepared by steam activation of char recovered as a solid by-product from tyre gasification; 27.5 g of the char was put in an alumina crucible and heated in an electric furnace from room temperature to 1000 °C at 7 °C/min. The steam was produced in a boiler heated at 200 °C and pumped into the reactors through a peristaltic pump at a steam flow rate of 148 ml/min. The steam was fed to the reactor once the final temperature was reached. The activation time at 1000 °C was of

Table 10
Results of steam activation of tyre char and comparison with data from the literature

	Charring conditions	Activation conditions (°C, h)	Chemical treatment	Activation gas flow rate (ml/min)	Burn–off (% w/w)	Bet area (m^2/g)	Bet area[a] (m^2/g)	Yield (%)
This work	Steam Gasif. 850 °C	1000, 3	Steam	148	77	548	620	9.5
Cunliffe et al.	Pyrolysis 450 °C	935, –	Steam	146	64	–	640	13.6
Sun et al.	Pyrolysis 600 °C	900, 1	Steam	500	–	1031	–	–
		850, 3	Steam	500	–	888	–	–
Merchant et al.	Pyrolysis 530 °C	920, 1	Steam	342	65	607	–	12.3
		850, 1.3	Steam	343	52.5	553	–	16.6
Ariyadejwanich et al.	Pyrolysis 500 °C	850, 4	Steam	680	77.5	–	1119	7.9

[a] Acidic demineralisation applied.

180 min. Table 10 shows the data for the activation, compared with some references from the literature (Mui et al., 2004).

The burn-off is calculated from the following relation:

$$\text{Burn off}(\%) = (w_1 - w_2/w_1) * 100$$

where w_1 is the initial dry mass of char, and w_2 is the final dry mass of the char after activation.

The two works reported in the table show an improved specific surface area by using an acidic demineralisation process. The data from this study are very similar to the results of Cunliffe, with respect to both the BET values and the yield of activated carbon. On the other hand, the specific surface area values of the other authors seem to be more dependent on the process parameters, in particular the temperature and the amount of activating agent.

4. Conclusions

This paper presents a comparative study of the steam gasification process, applied to three different waste typologies (RDF, poplar wood, and scrap tyres) and has the aim of comparing the corresponding yields and product compositions and exploring the most valuable uses of the by-products. The gasification conditions for the three materials were exactly the same, which allows for accurate comparisons of the performances of these raw materials. Furthermore, the experimental tests were conducted in rotary kilns, which have not been widely employed for gasification treatment; these kilns offer flexible configurations to easily manage of the process, even with a highly heterogeneous material, and are hardly found in literature.

The experimental data clearly show that, holding all the operational parameters constant, the yields and compositions of the resulting process fractions are largely influenced by the nature of the starting material.

All the materials show a comparable gas production, expressed as m^3 of gas/kg of feed; nevertheless, for RDF and poplar the conversion is very high (86%) (Turn et al., 1998), for tyres the process needs to be pushed towards a higher gas production.

The characteristics of the solid residues (char) coming from poplar and tyres suggest using them as raw materials for later processes, avoiding any reduction of the carbon content through further gas production. In this way, a satisfactory compromise between a good yield in hydrogen rich gas and a good char may be obtained. On the other hand, char derived from RDF showed high ash content, which suggested pushing the gasification conditions towards the maximum gas yield.

With the adopted process conditions, syngas from tyres has the highest hydrogen content, the highest yield of methane, ethylene, and ethane, and the lowest yield of oxygenated products (in agreement with the nature of the material). Syngas from poplar shows a diametrically opposed situation, with the maximum yield of CO and CO_2 and the lowest yield of methane and ethylene. Syngas from RDF shows intermediate values of all fractions. With respect to the suitable exploitation of the syngas, the heating value is always low, apart from the syngas from tyres, and is comparable to a poor gaseous fuel.

The possible exploitations of syngas for fuel cell applications or as starting material for Fisher–Tropsch synthesis were discussed by considering the H_2/CO ratio. With respect to tyres, such a ratio favours fuel cell applications, whereas for poplar and RDF the results are not as clear. Therefore, upgrading the gas (just cleaning or water gas shift reaction) could allow its exploitation in both these processes. The tyre syngas represents the best choice for gas utilisation as a chemical source.

Furthermore, the possible applications for the produced char were explored, and include the valorisation as active carbon for tyre waste and silicon carbide synthesis for poplar.

In the first case, the superficial area was increased from 40 to 548 m^2/g; furthermore, acidic cleaning (Nakagawa et al., 2002) was found to be effective in raising the superficial area further (to 620 m^2/g). In the second case, the synthesis of silicon carbide was explored, producing a ceramic powder which holds the same complex structure as the starting poplar and rendering the production of ceramic materials with organic morphologies feasible (Qian and Jin, 2006).

References

Banyasz, J.L., Li, S., Lyons-Hart, Shafer, J.K.H., 2001. Gas evolution and the mechanism of cellulose pyrolysis. Fuel 80, 1757–1763.
Bassilakis, R., Carangelo, R.M., Wojtowicz, M.A., 2001. TG–FTIR analysis of biomass pyrolysis. Fuel 80, 1765–1786.
Belgiorno, V., De Feo, G., Rocca, Della, Napoli, R.M.A., 2003. Energy from gasification of solid wastes. Waste Manage. 23, 1–15.
Braekman-Danheux, C., D'haeyere, A., Fontana, A., Laurent, P., 1998. Upgrading of waste derived solid fuel by steam gasification. Fuel 77 (1/2), 55–59.
Bridgwater, A.V., 2003. Renewable fuels and chemicals by thermal processing of biomass. Chem. Eng. J. 91, 87–102.
Casu, S., Galvagno, S., Calabrese, A., Casciaro, G., Martino, M., Russo, A., Portofino, S., 2005. Refuse derived fuels pyrolysis. Influence of process temperature on yield and products composition. J. Therm. Anal. Calorim. 80, 477–482.
Chaudhari, S.T., Bej, S.K., Bakhshi, N.N., Dalai, A.K., 2001. Steam gasification of biomass-derived char for the production of carbon monoxide-rich synthesis gas. Energ. Fuel 15, 736–742.
Cozzani, V., Petarca, L., Tognotti, L., 1995. Devolatilization and pyrolysis of refuse derived fuels: characterization and kinetics modelling by a thermogravimetric and calorimetric approach. Fuel 75, 903–912.
Effendia, A., Hellgardta, K., Zhanga, Z.G., Yoshida, T., 2005. Optimising H_2 production from model biogas via combined steam reforming and CO shift reactions. Fuel 84, 869–874.
Elordi, G., Olazar, M., Aguado, R., Lopez, G., Arabiourrutia, M., Bilbao, J., 2007. Catalytic pyrolysis of high density polyethylene in a conical spouted bed reactor. J. Anal. Appl. Pyrol. 79 (1–2), 450–455.

Encinar, J.M., Gonzalez, J.F., Gonzalez, J., 2002. Steam gasification of Cynara cardunculus L.: influence of variables. Fuel Process. Technol. 75, 27–43.
Esposito, L., Sciti, D., Piancastelli, A., Bellosi, A., 2004. Microstructure and properties of porous b-SiC templated from soft woods. J. Europ. Ceram. Soc. 24, 533–540.
Franco, C., Pinto, F., Gulyurtlu, I., Cabrata, I., 2003. The study of reactions influencing the biomass steam gasification process. Fuel 82, 835–842.
Franco, A., Giannini, N., 2005. Perspectives for the use of biomass as fuel in combined cycle power plants. Int. J. Therm. Sci. 44, 163–177.
Fujisawa, M., Hata, T., Bronsveld, P., Castro, V., Tanaka, F., Kikuchi, H., Furuno, T., Imamura, Y., 2004. SiC/C composites prepared from wood-based carbons by pulse current sintering with SiO_2: electrical and thermal properties. J. Euro. Ceram. Soc. 24, 3575.
Galvagno, S., Casu, S., Casabianca, T., Calabrese, A., Cornacchia, G., 2002. Pyrolysis process for the treatment of scrap tyres: preliminary experimental results. Waste Manage. 22, 917–923.
Galvagno, S., Casu, S., Casciaro, G., Martino, M., Russo, A., Portofino, S., 2006. Steam gasification of refuse-derived fuel (RDF): influence of process temperature on yield and product composition. Energ. Fuel 20, 2284–2288.
Galvagno, S., Casu, S., Martino, M., Di Palma, E., Portofino, S., 2007. Thermal and kinetic study of tyre waste pyrolysis via TG-FTIR-MS analysis. J. Therm. Anal. Calorim. 88, 1–8.
Garcia, A.N., Marcilla, A., Font, R., 1995. Thermogravimetric kinetic study of the pyrolysis of municipal solid waste. Thermochim. Acta 254, 277–304.
González, J.F., Encinar, J.M., González-Garcıa, C.M., Sabio, E., Ramiro, E., Canito, J.L., Ganán, J., 2006. Preparation of activated carbons from used tyres by gasification with steam and carbon dioxide. Appl. Surf. Sci. 252, 5999–6004.
Greil, P., Lifka, T., Kaindl, A., 1998. Biomorphic cellular silicon carbide ceramics from wood. I. Processing and microstructure. J. Eur. Ceram. Soc. 18, 1961–1974.
Hamelinck, C.N., Faaij, A.P.C., den Uil, H., Boerrigter, H., 2004. Production of FT transportation fuels from biomass; technical options, process analysis and optimisation, and development potential. Energy 29 (11), 1743–1771.
Helsen, L., Van den Bulck, E., 2005. Review of disposal technologies for chromated copper arsenate (CCA) treated wood waste, with detailed analyses of thermochemical conversion processes. Environ. Pollut. 134, 301–314.
Hwang, I.H., Matsuto, T., Tanaka, N., Sasaki, Y., Tanaami, K., 2007. Characterization of char derived from various types of solid wastes from the standpoint of fuel recovery and pretreatment before landfilling. Waste Manage. 27, 1155–1166.
Jess, A., 1996. Mechanism and kinetics of thermal reactions of aromatic hydrocarbons from pyrolysis of solid fuels. Fuel 75 (12), 1441–1448.
Kagann, R.H., 1982. Infrared absorption intensities for OCS. J. Mol. Spectrosc. 94, 192–198.
Kamo, T., Takaoka, K., Otomo, J., Takahashi, H., 2006. Production of hydrogen by steam gasification of dehydrochlorinated poly(vinyl chloride) or activated carbon in the presence of various alkali compounds. J. Mater. Cycles Waste Manage. 8, 109–115.
Kim, J.-W., Myoung, S.-W., Kim, H.-C., Lee, J.-H., Jung, Y.-G., Jo, C.-Y., 2006. Synthesis of SiC microtubes with radial morphology using biomorphic carbon template. Mater. Sci. Eng. A 434, 171–177.
Kingetsu, T., Ito, K., Takehara, M., 1998. High temperature phase and morphological changes of CVD–SiC films studied using in situ X-ray diffractometry. Mater. Lett. 36, 284–289.
Kiran, N., Ekinci, E., Snape, C.E., 2000. Recyling of plastic wastes via pyrolysis. Res. Conserv. Recy. 29, 273–283.
Ko, D.C.K., Mui, E.L.K., Lau, K.S.T., McKay, G., 2004. Production of activated carbons from waste tire – process design. Waste Manage. 24, 875–888.
Krishnarao, R.V., Subrahmanyam, J., 1996. Formation of SiC from rice husk silica–carbon black mixture: effect of rapid heating. Ceram. Int. 22, 489–492.
Krstic, V.D., 1992. Production of fine, high-purity beta Silicon Carbide powders. J. Am. Ceram. Soc. 75 (1), 170–174.
Leung, D.Y.C., Wang, C.L., 1998. Kinetic study of scrap tyre pyrolysis and combustion. J. Anal. Appl. Pyrol. 45, 153–169.
Lobachyov, K.V., Richter, H.J., 1998. An advanced integrated biomass gasification and molten fuel cell power system. Energ. Convers. Manage. 39 (16–18), 1931–1943.
Lu, R., Purushothama, S., Hyatt, J., Pan, W.-P., Riley, J.T., Lloyd, W.G., Flynn, J., Gill, P., 1996. Co-firing high-sulphur coals with refuse-derived-fuel. Thermochim. Acta 284, 161–177.
Lu, R., Purushothama, S., Yang, X., Hyatt, J., Pan, W.-P., Riley, J.T., Lloyd, W.G., 1999. TG/FTIR/MS study of organic compounds evolved during the co-firing of coal and refuse-derived fuels. Fuel Process. Technol. 59, 35–50.
Malkow, T., 2004. Novel and innovative pyrolysis and gasification technologies for energy efficient and environmentally sound MSW disposal. Waste Manage. 24, 53–79.
Mayoral, M.C., Izquierdo, M.T., Andrès, J.M., Rubio, B., 2001. Different approaches to proximate analysis by thermogravimetry analysis. Termochim. Acta 370, 91–97.
McKendry, P., 2002. Energy production from biomass (part 2): conversion technologies. Bioresource Technol. 84, 47–54.
Morf, P., Hasler, P., Nussbaumer, T., 2002. Mechanism and kinetics of homogeneous secondary reactions of tar from continous pyrolysis of wood chips. Fuel 81, 843–853.
Morris, M., Waldheim, L., 1998. Energy recovery from solid waste fuels using advanced gasifcation technology. Waste Manage. 18, 557–564.
Mui, E.L.K., Ko, D.C.K., Mc Kay, G., 2004. Production of active carbons from waste tyres – a review. Carbon 42, 2789–2805.
Nakagawa, K., Tamon, H., Suzuki, T., Nagano, S., 2002. Preparation and characterization of activated carbons from refuse derived fuel (RDF). J. Porous Mater. 9, 25–33.
Napoli, A., Soudais, Y., Lecomte, D., Castillo, S., 1997. Scrap Tyre pyrolysis: are the effluents valuable products? J. Anal. Appl. Pyrol., 373–382.
Pakdel, H., Pantea, D.M., Roy, C., 2001. Production of dl-limonene by vacuum pyrolysis of used tires. J. Anal. Appl. Pyrol. 57 (1), 91–107.
Porteous, A., 2001. Energy from waste direct combustion – a state of the art emissions review with an emphasis on public acceptability. Appl. Energ. 70, 157–167.
Qian, J.M., Wang, Ji.P., Jin, Z.H., 2004a. Preparation of biomorphic SiC ceramic by carbothermal reduction of oak wood charcoal. Mater. Sci. Eng. A 371 (1), 229–235.
Qian, J.M., Wang, J.P., Qiao, G.J., Jin, Z.H., 2004b. Preparation of porous SiC ceramic with a woodlike microstructure. J. Eur. Ceram. Soc. 24 (2), 3251–3259.
Qian, J.M., Jin, Z.H., 2006. Preparation and characterization of porous, biomorphic SiC ceramic with hybrid pore structure. J. Eur. Ceram. Soc. 26, 1311–1316.
Rodriguez-Reinoso, F., Molina-Sabio, M., Gonzalez, M.T., 1995. The use of steam and CO_2 as activating agents in the preparation of activated carbons. Carbon 33, 15–23.
Sharma, R.K., Wooten, J.B., Baliga, V.L., Hajaligol, M.R., 2001. Characterization of chars form biomass-derived materials: pectine chars. Fuel 80, 1825–1836.
Stenseng, M., Jensen, A., Dam-Johansen, K., 2001. Investigation of biomass pyrolysis by thermogravimetric analysis and differential scanning Calorimetry. J. Anal. Appl. Pyrol., 765–780.
Sujirote, K., Leangsuwan, P., 2003. Silicon carbide formation from pretreated rice husks. J. Mater. Sci. 38, 4739–4744.
Sullivan, J.D., Maier, C.J., Ralson, O.C., 1927. US Bur. Mines Tech. Pap., 384.
Sułkowski, W.W., Danch, A., Moczyński, M., Radon, A., Sułkowska, A., Borek, J., 2004. Thermogravimetric study of rubber waste-polyurethane composites. J. Therm. Anal. Cal. 78, 905.
Turn, S., Kinoshita, C., Zhang, Z., Ishimura, D., Zhou, J., 1998. An experimental investigation of hydrogen production from biomass gasification. Int. J. Hydrogen Energ. 23 (8), 641–648.
Varhegyi, G., Antal Jr., M.J., Jakab, E., Pyroska, S., 1997. Kinetic modelling of biomass pyrolysis. J. Anal. Appl. Pyrol. 42, 73–78.
Wang, J., Isida, R., Takarada, T., 2000. Carbothermal reactions of quartz and kaolinite with coal char. Energ. Fuels 14, 1108–1114.
Wesch, W., 1996. Silicon carbide: synthesis and processing. Nucl. Instrum. Meth. Phys. Res. B 116, 305–321.
Wie, L.G., Xu, S., Zhang, L., Liu, C., Zhu, H., Liu, S., 2007. Steam gasification of biomass for hydrogen-rich gas in a free-fall reactor. Int. J. Hydrogen Energ. 32, 24–31.
Wei, G.T.C., 1983. Beta SiC powders produced by carbothermic reduction of silica in high temperature rotary furnace. J. Am. Ceram. Soc. 66 (7), C111–C113.
Weimer, A.W., 1997. Carbide, nitride and boride materials. Synthesis and processing. Chapman & Hall-London.
Williams, P.T., Besler, S., 1995. Pyrolysis – thermogravimetric analysis of tyres and tyre components. Fuel 74, 1277–1283.
Xie, W., Pan, W.-P., Chuang, K.C., 2001. Thermal characterization of PMR polyimidies. Thermochim. Acta, 143–153.